computation

MDPI

Article

A Computerized Analysis of Flow Parameters for a Twin-Screw Compressor Using SolidWorks Flow Simulation

Ildiko Brinas [1,*], Florin Dumitru Popescu [1,*], Andrei Andras [1], Sorin Mihai Radu [1] and Laura Cojanu [2]

[1] Department of Mechanical, Industrial and Transport Engineering (IMIT), University of Petroșani, 332006 Petroșani, Romania; andrei.andras@gmail.com (A.A.); sorin_mihai_radu@yahoo.com (S.M.R.)
[2] Doctoral School in Mines, Oil and Gases, University of Petroșani, 332006 Petroșani, Romania; cojanulaura@gmail.com
* Correspondence: kerteszildiko@ymail.com (I.B.); fpopescu@gmail.com (F.D.P.)

Abstract

Twin-screw compressors (TSCs) are widely used in various industries. Their performance is influenced by several parameters, such as rotor profiles, clearance gaps, operating speed, and thermal effects. Traditionally, optimizing these parameters relied on experimental methods, which are costly and time-consuming. However, advancements in computational tools, such as Computational Fluid Dynamics (CFD) and Finite Element Analysis (FEA), have revolutionized compressor analysis. This study presents a CFD analysis of a specific model of a TSC in a 5 male/6 female lobe configuration using the SolidWorks Flow Simulation environment—an approach not traditionally applied to such positive displacement machines. The results visually present internal flow trajectories, fluid velocities, pressure distributions, temperature gradients, and leakage behaviors with high spatial and temporal resolution. Additionally, torque fluctuations and isosurface visualizations revealed insights into mechanical loads and flow behavior. The proposed method allows for relatively easy adaptation to different TSC configurations and can also be a useful tool for engineering and educational purposes.

Keywords: twin-screw compressor; SolidWorks; flow analysis; fluid dynamics; velocity; pressure distribution; heat transfer

check for updates

Academic Editors: Ali Cemal Benim, Jeffrey S. Marshall, Sergey A. Karabasov and Dimitris Drikakis

Received: 23 July 2025
Revised: 1 August 2025
Accepted: 4 August 2025
Published: 6 August 2025

Citation: Brinas, I.; Popescu, F.D.; Andras, A.; Radu, S.M.; Cojanu, L. A Computerized Analysis of Flow Parameters for a Twin-Screw Compressor Using SolidWorks Flow Simulation. *Computation* **2025**, *13*, 189. https://doi.org/10.3390/computation13080189

Copyright: © 2025 by the authors. Licensee MDPI, Basel, Switzerland. This article is an open access article distributed under the terms and conditions of the Creative Commons Attribution (CC BY) license (https://creativecommons.org/licenses/by/4.0/).

1. Introduction

Twin-screw compressors (TSCs) are a type of positive displacement machine. They are widely utilized in industrial applications for gas compression due to their high efficiency, reliability, and ability to handle a wide range of operating conditions [1–3]. These compressors consist of two intermeshing helical (screw) rotors—one male and one female—that rotate within a casing to trap and compress gas. Their compactness, simplicity, and ability to function efficiently at high speeds over a wide range of pressures and flow rates, while delivering continuous flow with minimal pulsations, make them a preferred choice in industries such as refrigeration, petrochemicals, and air compression. Unlike dynamic compressors, TSCs generate pressure by progressively reducing the enclosed volume between the inlet and outlet ports, a process determined by the machine's geometry [4]. They are available in both oil-injected and oil-free configurations, making them suitable for various industries, including refrigeration, petrochemicals, and manufacturing [5–7]. Extensive literature has been published on the behavior of these machines, dating back to the 1950s [8], continuing through the last decade, and up to the present day [9–11].

In recent years, significant advancements have been made in the design and performance optimization of compressors, requiring a deep understanding of fluid flow, thermodynamics, and mechanical interactions. Traditional methods of analysis and study for these machines have been extensively reviewed [12–14], concluding that experimental [15–17], theoretical [18–20], empirical, and semi-empirical methods [21–23] facilitate flow visualization, improve understanding of internal compressor phenomena, and provide valuable benchmark data for numerical modeling improvements [24–26]. However, as noted in [27], these methods have certain limitations—primarily due to the complexity of internal flow dynamics within compressors—and can be costly and time-consuming.

The limitations of traditional methods, combined with advancements in technology and computing power, have led to the growing adoption of computational analysis techniques and method. Several computational methods have revolutionized the study of twin-screw compressors by providing detailed insights into fluid dynamics, mechanical behavior, and thermodynamics, including the following:

1. Computational Fluid Dynamics (CFD) is widely used to study flow behavior, pressure distribution, and heat transfer inside twin-screw compressors. Various commercial and open-source software packages enable in-depth transient flow and heat transfer analyses, turbulence modeling, and leakage flow prediction.
2. Finite Element Analysis (FEA) is primarily used to assess the mechanical integrity and structural performance of twin-screw compressors, including rotor deformation studies, thermal stress analysis, fatigue analysis, and reliability studies.
3. Artificial Intelligence (AI) and Machine Learning (ML) are emerging as powerful tools for optimization and predictive modeling. These methods utilize advanced coding frameworks such as Python (TensorFlow, Scikit-learn) and MATLAB's Neural Network Toolbox.

All the described computational methods were thoroughly revised [28–30], concluding that although intensive research has been carried out, there is still room for further investigation. As mentioned, the computational approach to the research topic involves several techniques and software solvers. In CFD, pioneering work was conducted by Kovacevic [31,32] who introduced the method of block-structured grids for deforming domains and further improved it to create a single-domain type mesh, thus obtaining more accurate CFD simulation results.

Basha et al. [33] used ANSYS Fluent to model an oil-injected twin-screw compressor, employing a numerical mesh generated by SCORG (Screw Compressor Rotor Grid Generator) and its own developed interface. The work of Rane et al. [34] explores advancements in computational grid generation for analyzing fluid flow and thermodynamics in twin screw machines using CFD, demonstrating SCORG's adaptability for non-conventional rotor designs and illustrating its effectiveness in detailed flow analysis and design.

The study by Yeoh et al. [35] evaluated the performance of various interface capturing methods in CFD codes, particularly ANSYS Fluent and CFX, using case studies to highlight their strengths and limitations. Andres et al. [36] performed a CFD analysis of a two-stage twin-screw compressor, combining ANSYS CFX with a Fortran routine to highlight leakage flows and validate the simulation results against experimental data. Malael et al. [37] conducted a multi-flow numerical analysis of a screw compressor using TwinMesh for grid generation and ANSYS CFX for solving the flow equations.

Chamoun et al. [38] took a different approach, developing a mathematical model of the thermodynamic process in twin-screw compressors using Modelica for transient simulations, highlighting the necessity of water injection to prevent compressor failure and enhance efficiency. Papes et al. [39] developed an in-house code to define the motion of

the deforming mesh for a three-dimensional CFD analysis of an oil-injected twin-screw expander, providing insights into its thermodynamic behavior and efficiency.

Di Mattia et al. [40] proposed a novel modeling technique focused on thermodynamic analysis and reduced-order modeling of twin-screw compressors, implemented in Simulink with properties calculated using the CoolProp C++ library, demonstrating improved accuracy and performance. Xueming et al. [41] combined Gambit for fluid model generation with ANSYS Fluent to simulate the dynamic characteristics of flow domains, assessing the impact of design parameters and operating conditions on compressor performance.

Byeon et al. [42] employed a three-dimensional CFD analysis to evaluate the performance of a 4 × 6 oil-free twin-screw compressor using the commercial software Star-CCM+, yielding accurate pressure distributions and insightful graphical depictions. The research of Casari et al. [43] introduced new libraries to enhance solver capabilities and explored various dynamic meshing techniques within the open-source CFD software OpenFOAM for simulating positive displacement machines, particularly single- and twin-screw compressors, demonstrating OpenFOAM as a cost-effective alternative to commercial CFD software.

Further studies utilized different tools. Bojko et al. [44] applied ANSYS Polyflow and Fluent to simulate twin-screw pump performance using the non-Newtonian power law for fluid viscosity. Dragan et al. [45] developed a fully viscous 3D CFD methodology coupled with Artificial Neural Networks and Genetic Algorithms to optimize compressor rotor geometry using Numeca FINE/Design 3D.

Aydın et al. [46] conducted advanced rotor profiling and port optimization using SCORG-generated meshes and ANSYS CFX multiphase solvers to validate the performance optimization of compressors. Lyu et al. [47] developed an in-house code named Cavitating Dynamic Mesh (CDM) solver to perform a two-phase fluid flow analysis of the complex interactions between the working fluid's phases, providing insights into optimizing the efficiency and reliability of twin-scroll compressors and expanders.

The reviewed computational methods demonstrate significant advancements in the numerical modeling of twin-screw machines, particularly through the integration of CFD solvers, grid generation techniques, and optimization algorithms. The literature highlights a wide range of approaches, from structured meshing methods and commercial software applications to in-house code developments and advanced optimization frameworks. However, there is no single standard or universally accepted software for performing these analyses.

This study aims to present a flow analysis of a twin-screw compressor using SolidWorks 2023. While this commercial software is primarily used for model construction, it also allows CFD simulations. Its Flow Simulation Module has been applied in CFD analyses of axial compressor blades [48], high-pressure compressor blades [49], and gas separators [50], but not for twin-screw compressors. In this context, the present study introduces a novel approach for this type of analysis. The choice of this particular software is also based on the extensive experience of the research team in simulating various engineering phenomena using SolidWorks [51–53]. The study has been structured to facilitate replication and adaptation to different compressor configurations. The obtained results—covering fluid dynamics, pressure distribution, heat transfer, and velocity—align well with findings from other studies using different commercial software such as ANSYS Fluent/CFX [54,55], OpenFOAM, Simerics-SCORG, or other software [43,56]. The proposed method can also be further developed and applied to more complex models of TSCs.

To summarize, this study presents a novel application of SolidWorks Flow Simulation for analyzing the internal flow dynamics of a TSC. It contributes by demonstrating the feasibility and effectiveness of this approach for both educational and preliminary design

purposes, supported by a time-dependent CFD model of a 5/6 lobe TSC and validated through comparison with studies in the literature.

Unlike existing CFD studies using specialized tools, this research uses a widely accessible CAD-integrated solver, making advanced TSC analysis more approachable. Additionally, it reveals reverse flow effects, torque fluctuation patterns, and flow asymmetries that can influence design considerations.

After the extensive literature review section (1), the research is structured as follows: (2) theoretical aspects regarding twin-screw compressors; (3) creation of the virtual model and flow simulation, and (4) results and discussions on volume, flow trajectory, temperatures, and pressures obtained.

2. Theoretical Aspects Regarding TSC

The standard layout of a TSC is shown in Figure 1 and consists of two counter-rotating helical rotors housed within a compressor casing. Gas intake and discharge occur through nozzles located generally at opposite ends of the compressor. The rotors can be designed to have three, four, or five lobes.

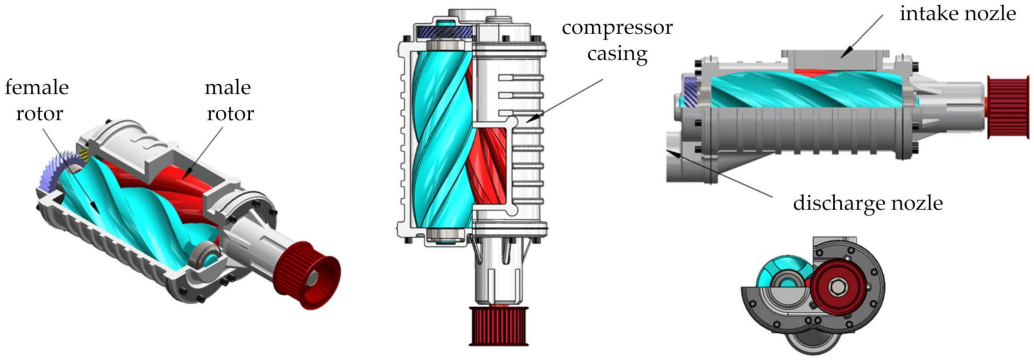

Figure 1. Standard layout of a TSC with corresponding parts.

The TSC is a positive displacement machine that operates in three distinct phases: suction, compression, and discharge. TSC operation can be described by presenting the working mode for a single phase involving only one lobe of the male rotor and the inter-lobe space corresponding to the female rotor. This allows extrapolation of the relative interaction of all lobes and inter-lobe spaces, resulting in a uniform, non-pulsating, and continuous gas flow through the compressor.

The suction phase is illustrated in Figure 2a. As the male rotor starts the rotation, between its lobe, an inter-lobe space appears in the area of the female rotor where vacuum is formed and gas is drawn in through the intake port. As the rotors continue to rotate, the space between the lobes increases, and the gas flows continuously into the inter-lobe space. Just before the inter-lobe space moves out of alignment with the intake port, the entire length of the inter-lobe space is open from one end to the other, so that the lobes and the space between them are completely unmeshed. In this way, the inter-lobe space is fully filled with the aspirated gas.

There is also a transitional phase between suction and compression where the aspirated gas is enclosed within the inter-lobe space, isolated from both the intake and discharge ports, and is simply transported radially at a constant rotational speed, maintaining the suction pressure.

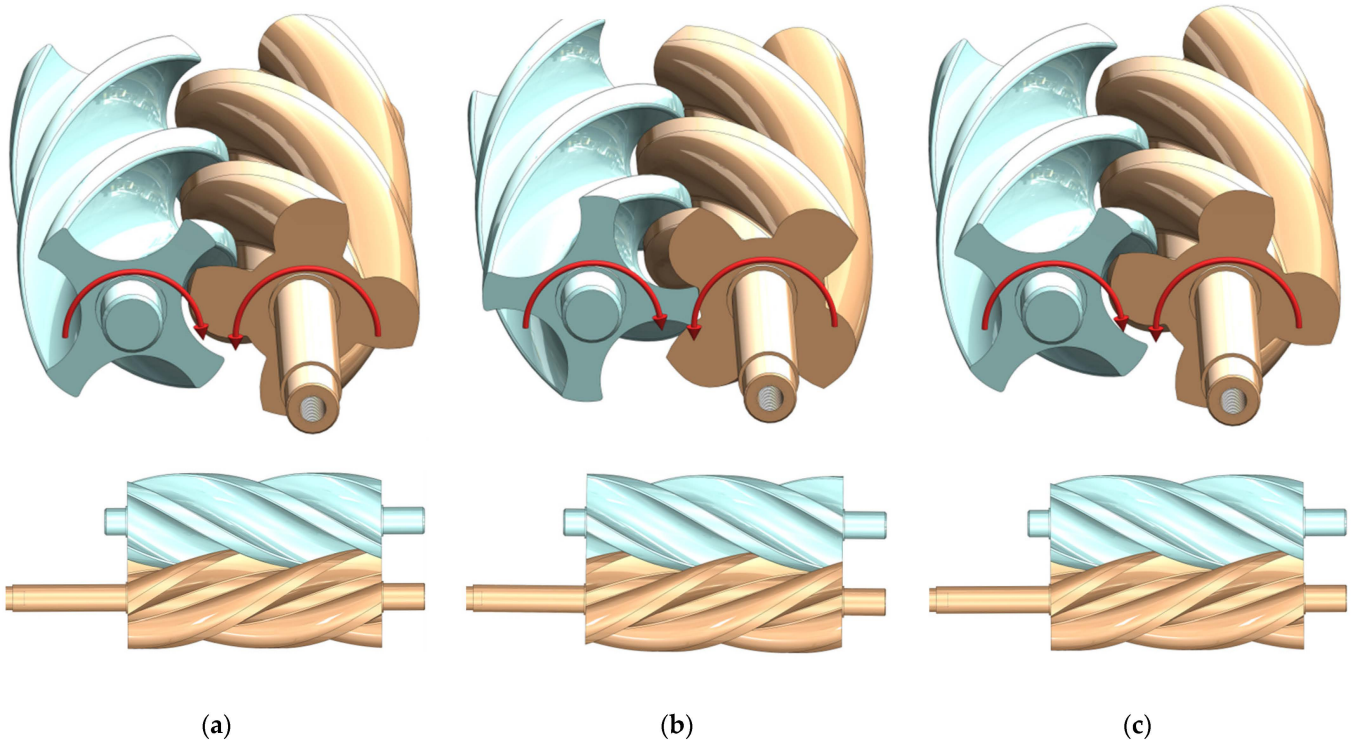

(**a**) (**b**) (**c**)

Figure 2. Visual representation of the working cycle of a TSC. (**a**) Suction phase: gas enters through intake, filling the inter-lobe space; (**b**) Compression phase: intake is closed, and the inter-lobe volume is reduced; thus, the gas pressure increases; (**c**) Discharge phase: final pressure is reached, and compressed gas is expelled.

Figure 2b illustrates the compression phase, where the inter-lobe spaces corresponding to the next male rotor lobe are filled with gas near the suction end and compress the gas toward the discharge port. The sealing line (contact point) moves axially from the intake side to the discharge side. As a result, the volume occupied by the gas within the inter-lobe space is reduced, and consequently, the gas pressure increases.

Finally, the discharge phase is illustrated in Figure 2c. At a certain point during the rotation of the rotors—depending on their design and the compression ratio—the discharge port is uncovered, and the compressed gas is expelled through the inter-lobe space formed by the merging lobes. It can be summarized that, over time, the sealing line of a pair of lobes moves axially, while simultaneously, another quantity of gas is introduced into a different inter-lobe space, thereby repeating the working phases of the compressor cycle.

In the industry, mainly two different types of screw compressors can be used:

- Dry screw compressors;
- Liquid-injected screw compressors, which can be further divided into oil-injected machines and machines that use other types of liquids.

Dry screw compressors typically use gear drives mounted on shafts to keep the two rotors in correct alignment. They are suitable for aeration services in the pharmaceutical industry, high-purity chemical industry, and other applications where the complete absence of contaminants in the discharged air is essential.

Oil-injected screw compressors are generally built without timing gears. For compressors using other liquid injection types, timing gears are usually necessary to maintain counter-rotation of the two screws. The injected liquid may be water, a heat-transfer fluid, or another type of liquid. In oil-injected compressors, the lubricant forms a film that separates the profiles of the two screws when one rotor drives the other.

2.1. General Operating Principles

A high-performance screw compressor can be assimilated to a rotary piston consisting of two shafts designed to combine displacement with internal compression. The intake fluid/gas is transported toward the discharge port. It is enclosed in continuously shrinking spaces located between the lobes of the two helical rotors. The result is the compression of the fluid/gas to the final pressure before being discharged.

The position of the discharge port limit determines the built-in volume ratio v_i, which represents the ratio between the volume of the gas mass at discharge and that at intake. The corresponding built-in compression ratio π_i represents the pressure of the gas at discharge relative to the intake pressure and is calculated using the following equation:

$$\pi_i = v_i^k \tag{1}$$

where k is the ratio of the specific heats of the gas at constant pressure and volume.

The compression process is illustrated in the theoretical pressure–volume diagram shown in Figure 3. Generally, a rotary screw compressor is designed for a specific compression ratio. If it discharges into a receiver with a compression ratio higher than the built-in one π_i, then the compressor and its end wall will be exposed to that pressure. When operating at compression ratios higher than those for which they were designed, they experience a reverse gas flow that causes a significant drop in machine performance. Screw compressors, on the other hand, are only constrained by the strength of the machine components and the input power. For this reason, these compressors can easily produce high compression ratios, generating high discharge pressures. Screw compressors can also operate at compression ratios lower than their design values, with the observation that this operating mode will result in reduced efficiency. This phenomenon is illustrated in Figure 3 by the shaded areas.

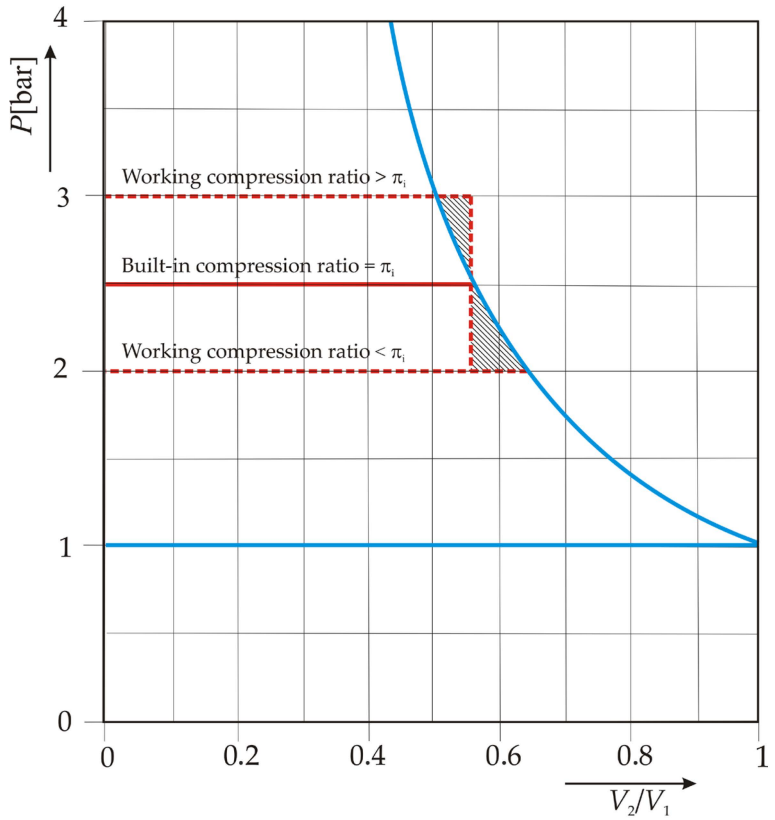

Figure 3. Pressure–volume (pV) diagram for a rotary screw compressor.

2.2. Equations of Conservation for the Volume Control and Auxiliary Equations

The working chamber of a screw machine is the internal space that contains the working fluid and represents a typical example of an open thermodynamic system in which the mass flow rate varies over time. Thus, suction and discharge can be defined through a control volume for which differential equations corresponding to the conservation laws of mass and energy are written. These equations are derived based on the Reynolds transport theorem.

A key feature of the presented model is the use of the variable flow energy equation to calculate thermodynamic and flow processes in a screw machine under conditions of varying rotational angle or time and to assess how these are influenced by changes in rotor profile geometry. In this context, internal energy (rather than enthalpy) becomes the dependent variable. This approach is more computationally convenient than using enthalpy, as internal energy can be derived without reference to pressure, even for real fluids. The calculation is performed iteratively until a convergent solution is reached. The desired pressure, which is an output variable, along with other thermodynamic properties, can be determined by differentiating the internal energy. The model uses the following conservation equations:

The conservation of internal energy equation is expressed as follows:

$$\omega\left(\frac{\mathrm{d}U}{\mathrm{d}\theta}\right) = \dot{m}_{in}h_{in} - \dot{m}_{out}h_{out} + \frac{\mathrm{d}Q}{\mathrm{d}t} - \omega p\left(\frac{\mathrm{d}V}{\mathrm{d}\theta}\right) \tag{2}$$

where U is the internal energy, θ is the rotational angle of the main rotor, ω is the angular velocity of rotation, $h = h(\theta)$ is the specific enthalpy, $\dot{m} = \dot{m}(\theta)$ is the mass flow rate, $p = p(\theta)$ is the fluid pressure in the working chamber, $Q = Q(\theta)$ is the heat transfer between the fluid and the compressor enclosure, and $V = V(\theta)$ is the local volume of the compressor's working chamber. In Equation (2), the subscripts in and out refer to the fluid flow at the compressor inlet and outlet, respectively.

The total fluid flow enthalpy is expressed as follows:

$$\dot{m}_{in}h_{in} = \dot{m}_{suc}h_{suc} + \dot{m}_{l,g}h_{l,g} + \dot{m}_{oil}h_{oil} \tag{3}$$

where l, g are indices referring to leakage through dispersion; *suc* indicates suction conditions; and *oil* denotes oil.

The total outlet enthalpy of the fluid is expressed as follows:

$$\dot{m}_{out}h_{out} = \dot{m}_{dis}h_{dis} + \dot{m}_{l,l}h_{l,l} \tag{4}$$

where indices l, l refers to leakage loss, and *dis* indicates the discharge conditions with $\dot{m}_{dis}$ denoting the discharge mass flow rate of the gas contaminated with the oil or other liquid injected.

The right side of the energy Equation (2) consists of the following terms that are modelled. The heat exchange between the fluid, the compressor rotors, and the casing with the external environment is determined by the temperature difference between the gas and the surfaces of the casing and rotor. This heat exchange can be evaluated using the appropriate heat transfer coefficient, expressed as $\mathrm{Nu} = 0.023 \times \mathrm{Re}^{0.8}$. For characteristic lengths and for the difference between the outer and inner diameters of the main rotor, different values for the Reynolds and Nusselt numbers were adopted. The characteristic velocity for the Reynolds number is calculated based on the local mass flow rate and the cross-sectional area. Thus, the surface area over which heat transfer occurs, as well as the wall temperature, depends on the rotational angle θ of the main rotor. The energy gain due to the gas flow into the working volume is represented by the product of the

mass inflow and its average enthalpy. As such, the energy flux varies with the rotational angle. During the suction period, gas enters the working volume, determining the average enthalpy of the gas in the suction chamber. During the periods when the suction port is closed, a certain amount of compressed gas leaks from the compressor's working chamber through clearances. The mass of this gas, as well as its enthalpy, are determined based on the gas leakage equations. The total inlet enthalpy is also affected by the amount of enthalpy introduced into the working chamber by the injected oil. The energy loss due to gas flowing out of the working volume is defined by the product of the mass flow rate and the average enthalpy of the gas. It should be noted that while leakage and heat exchange terms are retained in the model, both preliminary calculations and the studied literature [57,58] indicate these contribute less than 5–7% to the total energy variation under nominal operating conditions. During the discharge phase, this refers to the compressed gas entering the discharge port, while during expansion caused by discharge pressure, it refers to gas leaking through clearances from the working volume into an adjacent space at lower pressure. If the pressure in the working chamber is lower than in the discharge chamber and the discharge port is open, the flow will reverse direction, i.e., from the discharge port back into the working chamber. In this case, the mass transfer has a negative sign, and the assumed enthalpy is equal to the average enthalpy of the gas in the pressure chamber. From a thermodynamic perspective, the gas compression process is characterized by the expression $\left(p\frac{\mathrm{d}V}{\mathrm{d}\theta}\right)$. This expression is evaluated based on the local pressure and the variation of the local volume using relationships that define the screw rotor kinematics, which produce the instantaneous working volume and its change relative to the rotational angle θ. If oil or another fluid is injected into the compressor's working chamber, the oil mass flow and its enthalpy must be included as input parameters. Despite the oil mass fraction in the mixture being significant, its effect on the volumetric flow rate is limited, as the oil volume fraction is typically very small. The total mass flow of the fluid includes the injected oil, most of which remains mixed with the working fluid. Heat transfer between the gas and oil droplets is described by a first-order differential equation.

The mass continuity equation is expressed as follows:

$$\omega\frac{\mathrm{d}m}{\mathrm{d}\theta}h_{med} = \dot{m}_{in}h_{in} - \dot{m}_{out}h_{out} \tag{5}$$

where the mass inflow rate is composed of $\dot{m}_{in}h_{in} = \dot{m}_{suc} + \dot{m}_{l,g} + \dot{m}_{oil}$ and the mass outflow rate is composed of $\dot{m}_{out}h_{out} = \dot{m}_{dis} + \dot{m}_{l,l}$.

Each of the mass flow rates satisfies the continuity equation as follows:

$$\dot{m} = \rho \cdot w \cdot A \tag{6}$$

where w is the fluid velocity measured in m/s, ρ is the fluid density measured in kg/m^3, and A is the cross-sectional area of the flow measured in m^2.

The instantaneous density $\rho(\theta)$ is determined as the ratio between the instantaneous mass $m(\theta)$ contained in the control volume and the corresponding instantaneous volume $V(\theta)$, according to the relation $\rho(\theta) = m(\theta)/V(\theta)$.

The cross-section area A is determined by the geometry of the TSC and can be modeled by a periodic function dependent on the rotational angle θ. The area of the suction port can be defined by the following relation:

$$A_{suc} = A_{suc,0} \cdot \sin\left(\pi\frac{\theta}{\theta_{suc}}\right) \tag{7}$$

where the subscript index *suc* indicates the suction conditions for the initial value of the angle θ at the moment the suction port opens, and $A_{suc,0}$ represents the maximum cross-

sectional area of the suction port. The reference value of the rotational angle θ is considered at the closing of the suction port, so that suction ends at angle θ = 0.

Similarly, the area of the discharge port is defined by the following relation:

$$A_{dis} = A_{dis,0} \cdot \sin\left(\pi \frac{\theta - \theta_c}{\theta_e - \theta_s}\right) \tag{8}$$

where e is an index indicating the end of discharge, c is an index indicating the end of compression, and $A_{dis,0}$ represents the maximum cross-sectional area of the discharge port.

The fluid velocities at the suction and discharge ports are calculated using the following equation:

$$w = \mu\sqrt{2(h_2 - h_1)} \tag{9}$$

where μ is the flow coefficient of the suction or discharge port, and 1 and 2 are indices representing the downstream and upstream conditions of the respective port. If $h_2 < h_1$, a reverse flow will be calculated using the algorithm.

3. Modeling and Simulation

3.1. The Geometric Model of the Analysed TSC

The virtual model of the compressor was created using the SolidWorks software package. It is built as an assembly consisting of four parts, including the main rotor with five lobes, the secondary rotor with six lobes, the compressor base, and the cover, all build at real dimensions as shown in Figures 4–7.

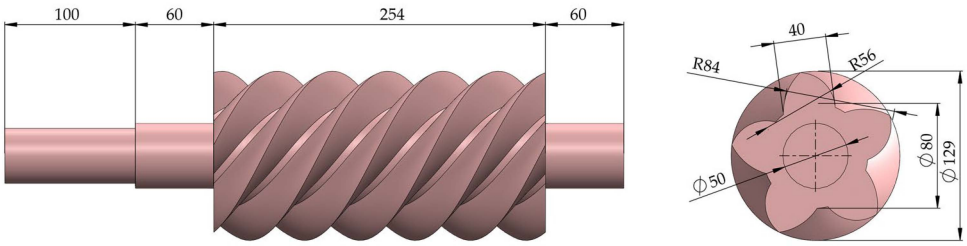

Figure 4. Model of the main rotor with five lobes.

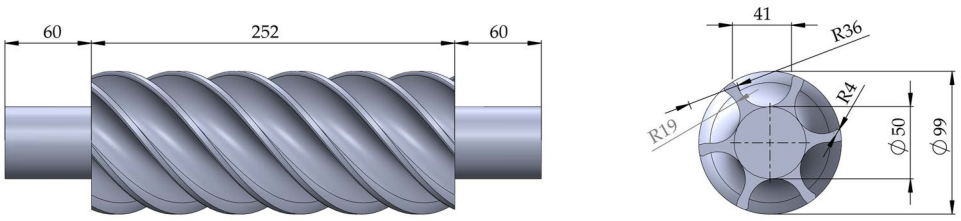

Figure 5. Model of the secondary rotor with six lobes.

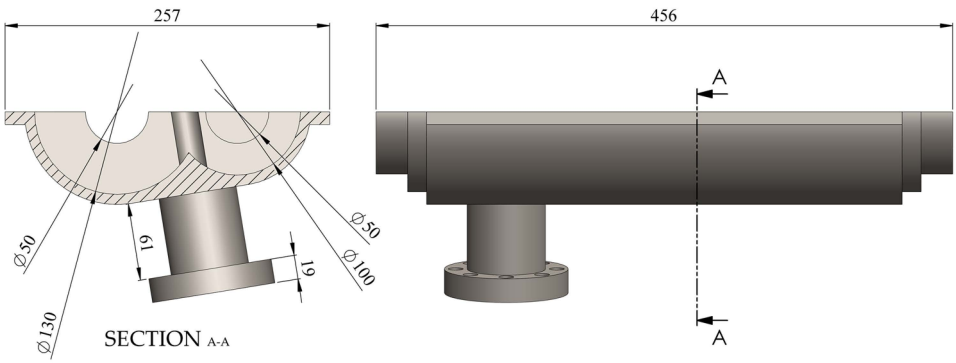

Figure 6. Model of the bottom of the TSC casing.

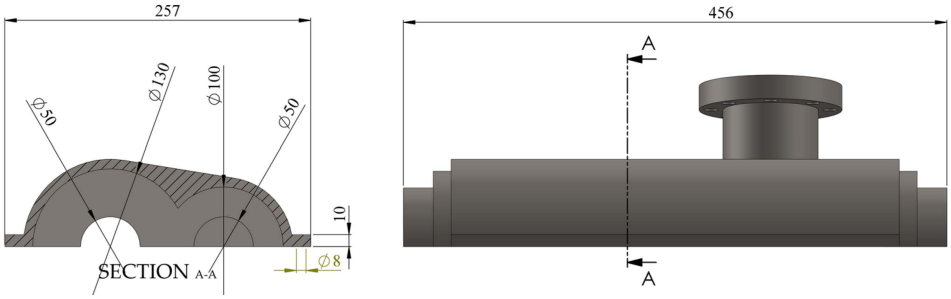

Figure 7. Model of the top cover of the TSC casing.

The 5/6 lobe configuration of a TSC was selected due to its widespread industrial application, being considered a standard in many commercial designs, and because of its favorable balance between volumetric efficiency and mechanical stability. This particular geometry also offers reduced inter-lobe space, which minimizes leakage losses and enhances compression performance compared to lower-lobe configurations. Additionally, the 5/6 arrangement provides smoother torque transfer and reduced pulsations, resulting in lower vibration and noise levels during operation. Its common use in both experimental and numerical studies also facilitates benchmarking and ensures that the findings of this work are representative of other screw compressor designs.

3.2. Computational Mesh Generation

The computational mesh was automatically generated by SolidWorks Flow Simulation using the following built-in curvature and proximity refinement options: the level of initial mesh was set to 5 (with possible values between 1 and 7), and the minimum gap size set to 0.01 m. These values were selected as optimal in terms of computational time and resource efficiency, based on a mesh sensitivity analysis performed at three refinement levels, which showed negligible variations in the output parameters.

It is important to note that SolidWorks Flow Simulation generates a computational mesh consisting of small hexahedaral elements (cells) with local non-conformal grid refinement levels, in combination with the so-called "smart cell" technique to treat curved boundaries, and uses the Finite Volume Method (FVM) on this basis.

The generation of the computational mesh with the above options resulted in a total of 198,252 cells in SolidWorks Flow Simulation. This value represents the total number of fluid cells into which the gas inside the TSC was discretized, as presented in Figure 8.

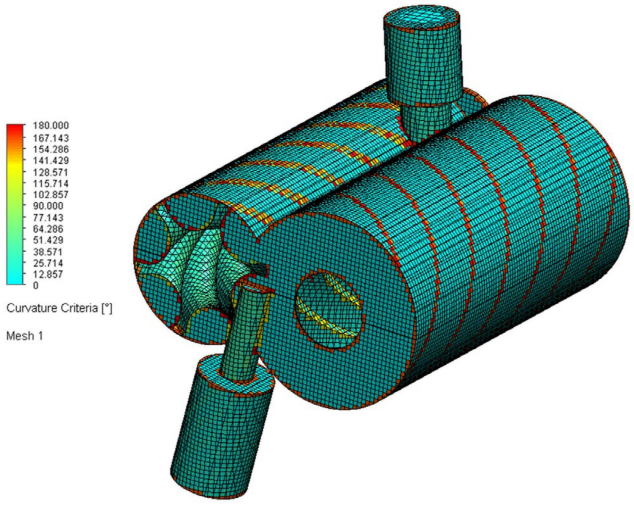

Figure 8. Representation of the obtained computational mesh with the total number of elements.

Out of the total, 107,069 are elements that discretize the contact between the gas and the solid surfaces of the TSC. These are referred to as fluid cells that contact solids in the solver. These are illustrated in Figure 9a for the contact between the gas and rotors and Figure 9b for the contact between the gas and the compression chamber wall.

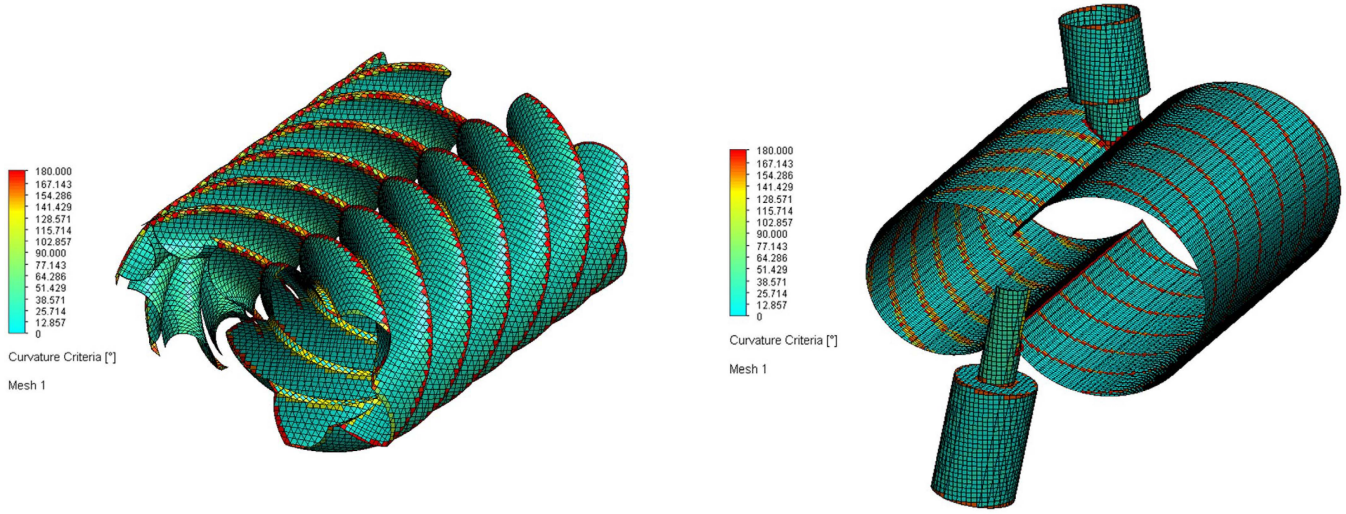

(**a**) (**b**)

Figure 9. Representation of the mesh elements discretizing the contact between the gas and the solid parts of the TSC: (**a**) contact with the rotors; (**b**) contact with the compression chamber wall.

3.3. Numerical Parameter Setup, Flow Simulation Using the Virtual Model, and Boundary Conditions

In order to run the simulation, several parameters were first defined. The fluid flow within the TSC was simulated using the transient time-dependent solver of SolidWorks Flow Simulation as an internal type, which solves the compressible Navier–Stokes equations. The working fluid was air treated as an ideal gas to account for density variations due to pressure and temperature changes. The simulation considered both laminar and turbulent flow regimes, with turbulence captured by the built-in k–ε model of the software solver. The analysis was unsteady, capturing the periodic nature of the compression cycle.

To represent the rotor motion, two sliding rotating domains were defined around the male and female rotors, with the geometry recognition parameter set to the CAD Boolean type. These domains are cylindrical regions that rotate relative to the stationary casing, allowing the solver to accurately model inter-lobe motion, dynamic sealing effects, and reverse flow events. The main rotor was assigned a speed of 500 RPM, while the female rotor rotated at 425 RPM in the opposite direction, maintaining the real kinematic ratio of the 5/6 lobe configuration.

For the compression chamber, the adiabatic wall type was chosen in order to minimize external heat transfer. As initial conditions, a pressure of 101,325 Pa and a temperature of 293.2 K were considered, with initial velocities V_x, V_y, and V_z considered zero. At the same time, a value of 2% for the turbulence intensity parameter and 0.00025 m for the turbulence length parameter were set. The time interval considered for simulation is 1 s.

The computational domain includes the internal volume of the compressor casing, which was isolated using virtual lids at the entrance and outlet ports, as shown in Figure 10.

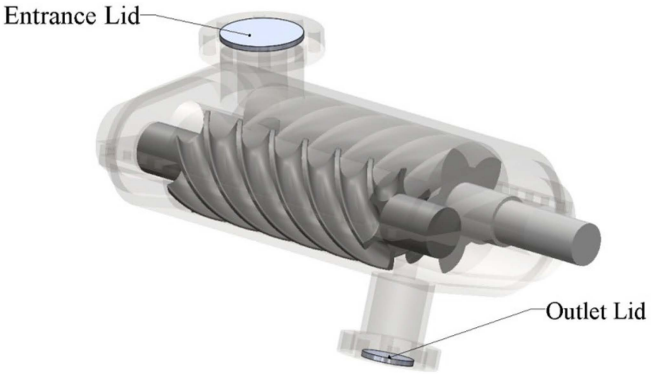

Figure 10. Enclosing of the internal volume of the mode for the flow simulation.

Three boundary conditions were defined for the simulation to ensure realistic operating conditions of the analyzed twin-screw compressor.

At the inlet, a volumetric flow rate of 0.005 m^3/s was imposed, with uniform flow normal to entrance lid/intake surface, a pressure of 101,325 Pa, and a temperature of 293.2 K. A turbulence intensity of 2% and a turbulence length of 0.0025 m were specified, which are typical values for moderately developed internal flows and ensure numerical stability without overestimating turbulence effects.

At the outlet, a total pressure of 300,000 Pa and a temperature of 313.2 K were applied, with the same turbulence parameters as at the inlet. The chosen discharge pressure corresponds to the nominal working point of the compressor, representing typical conditions for a 5/6 lobe TSC under standard load. This value ensures that the simulated pressure ratio is consistent with real-world industrial applications, while variations of up to ±20% may occur under different operational scenarios—such cases are intended for future parametric studies.

The walls of the compression chamber were modeled as real walls of the stator type (See Figure 11), with no-slip conditions and an adiabatic thermal boundary, meaning that no heat transfer occurs between the fluid and the external environment.

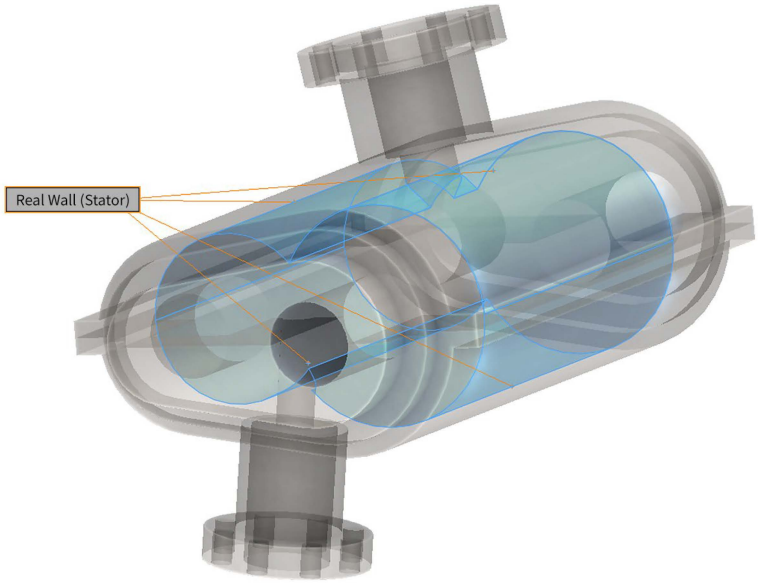

Figure 11. Compression chamber walls modelled as stator-type real walls.

4. Results and Discussion

As a result of the flow simulation, first the volume of fluid (air) inside the compressor chamber was determined with the aid of the "Check Geometry" option. This returns a fluid volume of 0.002521 m^3 inside the compressor, shown in Figure 12a as a complete three-dimensional part and in Figure 12b in a longitudinal cut-section view.

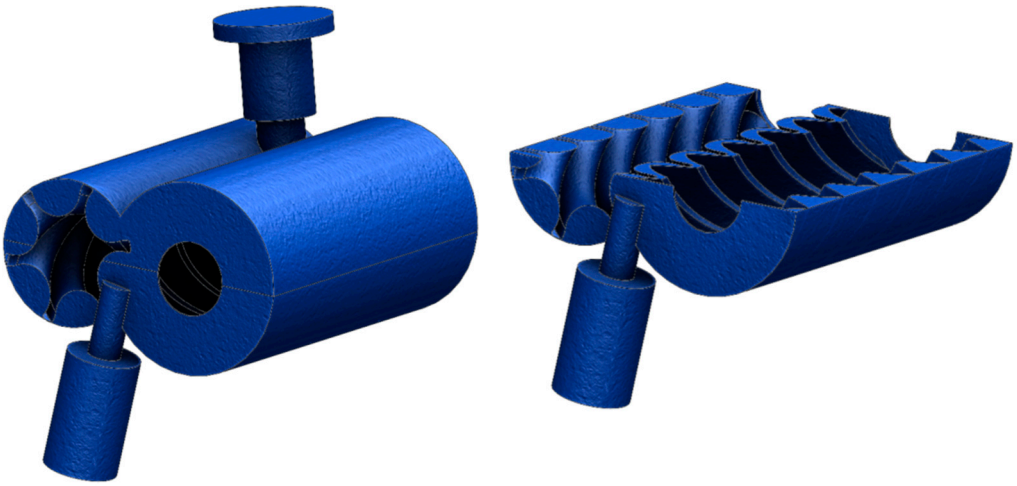

(**a**) (**b**)

Figure 12. Air volume inside the compressor chamber: (**a**) representation as a complete 3D part; (**b**) represented in a longitudinal cut-section view.

Next, the flow simulation results present the trajectory of fluid flow inside the compressor, with another parameter visually represented being the flow velocity in [m/s], presented in a three-dimensional view in Figure 13a and in cross-section in Figure 13b. The velocity field shown reveals high-speed regions near the rotor tips. These high velocities are associated with the tight clearances where leakage flows occur.

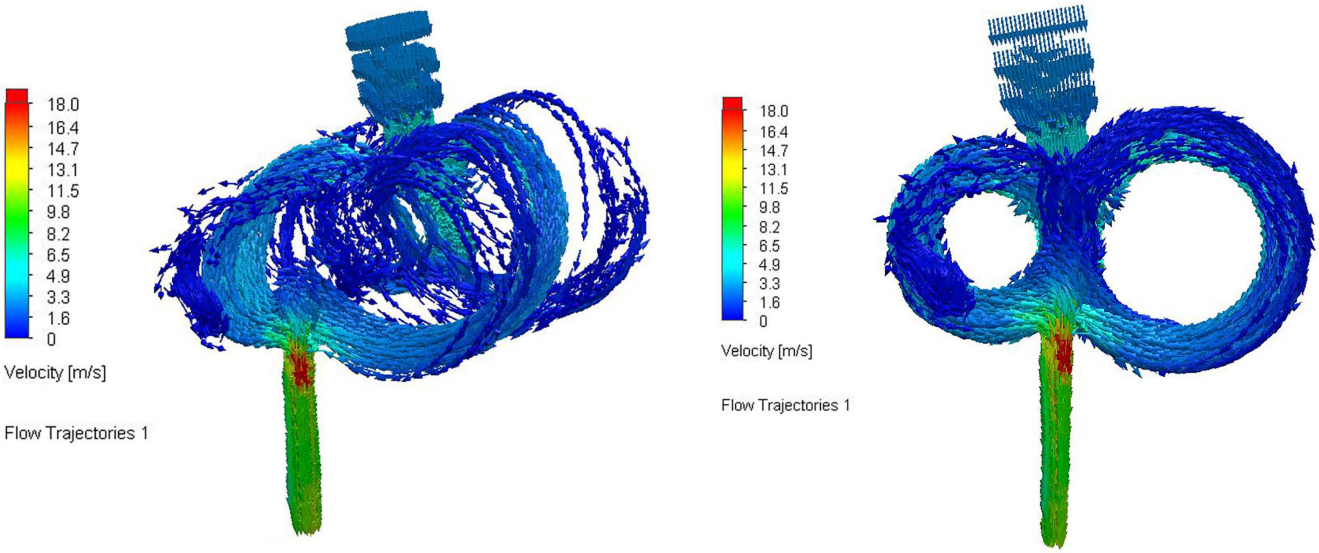

(**a**) (**b**)

Figure 13. Trajectory of the fluid flow with colored visual representation of velocity: (**a**) 3D view; (**b**) cross-section view.

Figure 14 reveals a reverse fluid flow situated near the discharge port, which—as previously discussed in Section 2 of the present study—occurs because the operating

discharge pressure exceeds the built-in compression ratio of the TSC. The arrows in the figure clearly represent the change of direction near the outlet. This backflow is a known phenomenon in screw compressors and indicates that some compression energy is being dissipated in reversing the flow direction.

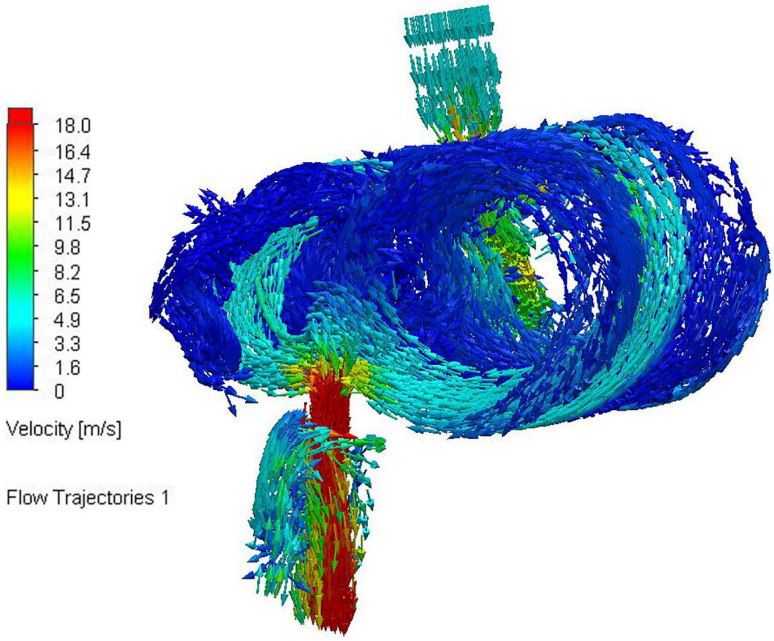

Figure 14. Reverse fluid flow trajectory near the outlet of the TSC.

In order to better understand the flow patterns and provide the clearest visual representation, SolidWorks Flow Simulation allows the user to create isosurfaces (also known as isolevels) for any physical property that is simulated. These are actually a powerful visualization tool in 3D space used to represent specific values of a physical property (like velocity, pressure, or temperature) across a 3D computational fluid flow domain, where that specific property or parameter has constant a value. In Figure 15, the variations of fluid velocity inside the compressor across 2000 isosurfaces is presented. The isosurface representation shows a gradual acceleration of the working fluid along the compression path.

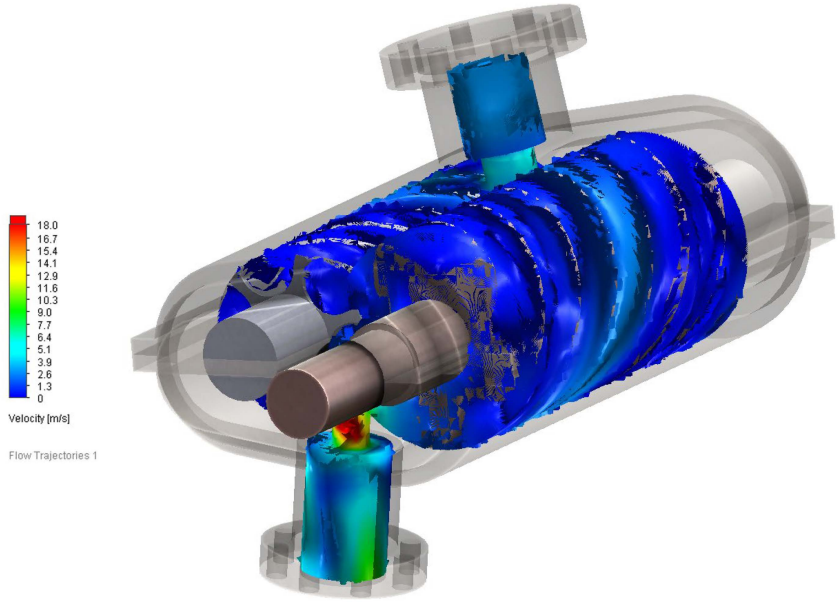

Figure 15. Variation of fluid velocity represented across 2000 isosurfaces.

Figure 16 details the variation of the fluid temperature inside the compressor across 15,000 isosurfaces, highlighting the thermal stratification caused by gas compression and leakage.

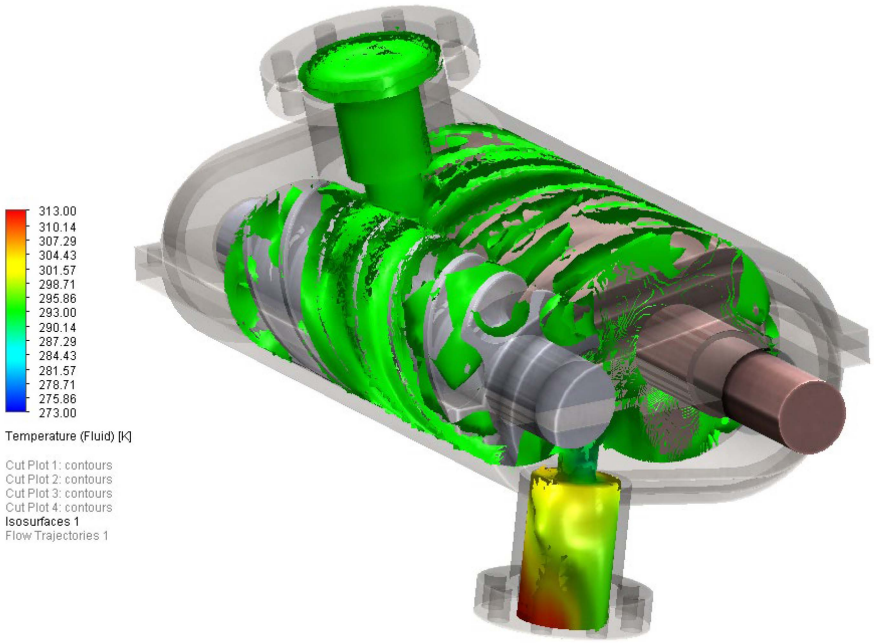

Figure 16. Temperature variation represented across 15,000 isosurfaces.

Finally, the results obtained based on flow simulation allow the representation of pressure variation at the outlet port, as shown in Figure 17 in a cross-section view. The localized pressure drops can be observed near the discharge port, corresponding to leakage paths and backflow.

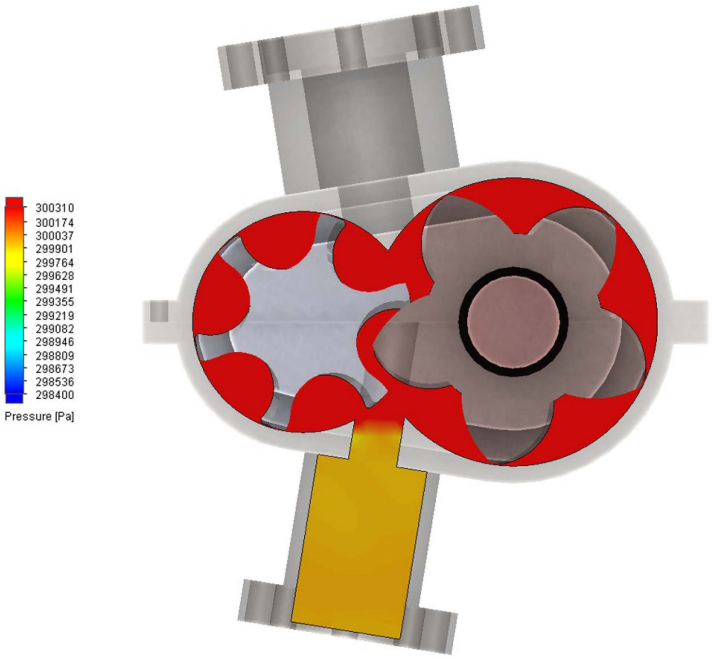

Figure 17. Pressure variation at the discharge port in cross-section view.

In SolidWorks Flow Simulation, several types of "goals" can be created and used, either to design the key objectives of a project/simulation, or to indicate when the simulated parameters have converged to a reasonable solution.

In the case of rotating components, such as the two rotors of the analyzed TSC, the "SGtorque" type goal was employed to determine the torque acting on the male and female rotor, separately. Figure 18a,b show the variation of the torque value during 1 s (corresponding to 1000 iterations in the simulation), allowing the representation of this parameter change over time under the flow conditions. The signs of the torques signifies they are opposite to the signs of the movement of the rotors. These torque variations illustrate the alternating mechanical loads on the male and female rotors. These oscillations result from periodic compression and leakage events as rotor lobes pass the suction and discharge ports.

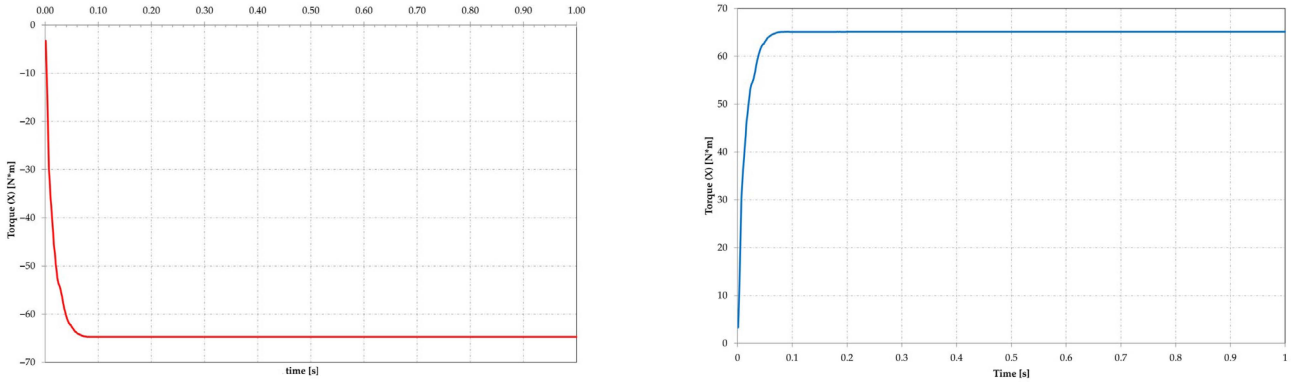

(**a**) (**b**)

Figure 18. Variation of torque acting on the rotors during 1 s (1000 iterations): (**a**) male rotor; (**b**) female rotor.

It is also important to mention that once the TSC reaches the nominal working regime and stabilizes, the torque is not constant at the approx. 65 Nm value, but has small variations around this value due to the nature of the compression process. This can be observed in Figure 19, where the peaks are visible between 65.103 and 65.108 Nm. This variation chart is also plotted for 1 s (1000 iterations), and the behavior is similar to both rotors. The figure highlights the small fluctuations (~±0.005 Nm) around the nominal torque value, which represents a characteristic of the pulsating pressure field inside the TSC.

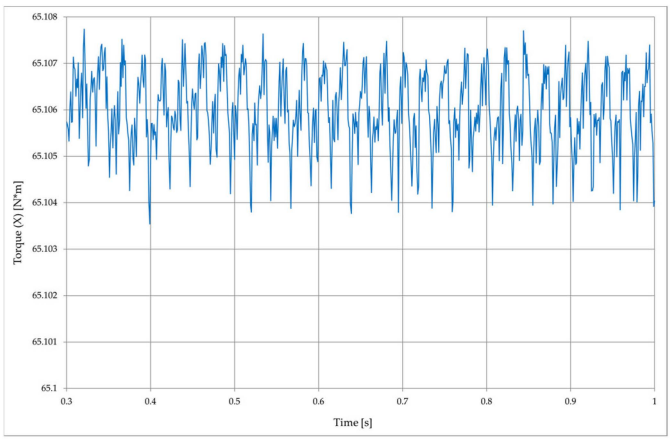

Figure 19. Detail of the torque small variation during the nominal working regime of the TSC.

Finally, an "SG Average Static Pressure" type goal was used to collect the static pressure values at the outlet, also for a duration of 1 s, in order to plot the variation of this parameter as presented in Figure 20. The figure illustrates the local pressure field within the discharge region and across the internal flow domain. This representation highlights the pressure

gradients and transient effects that occur near the outlet, which are not constant due to reverse flows and rotor-induced compression dynamics. The pressure distribution shown provides valuable insights into localized flow phenomena, such as fluctuations caused by the rotor motion, which are not directly constrained by the fixed boundary condition.

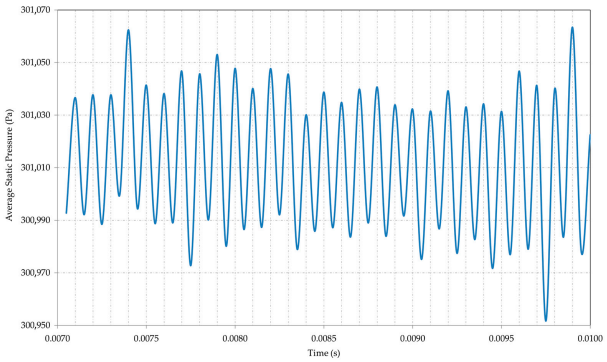

Figure 20. Variation of the average static pressure at the TSC outlet.

In order to validate the simulation outcome, the obtained results for the average outlet pressure, temperature rise, and torque were compared with published data from similar TSC studies conducted in ANSYS Fluent [54] and SCORG [55]. The comparison results show good agreement, with deviations within ±10%, indicating that the SolidWorks Flow Simulation approach provides reliable predictions for the studied configuration. Future work will focus on enhancing the accuracy and applicability of the proposed methodology by incorporating experimental or analytical validation. Additionally, the approach could be extended by benchmarking against one of the other CFD platforms such as ANSYS Fluent, OpenFOAM, and/or SCORG.

5. Conclusions

This study successfully demonstrated the feasibility of using SolidWorks Flow Simulation beyond the design modeling only, namely for performing detailed CFD analysis of a twin-screw compressor, a domain traditionally reserved for more specialized tools such as ANSYS Fluent, SCORG, or OpenFOAM.

The major findings are as follows:

- Simulation Reliability: The internal flow structures, including suction, compression, and discharge phases, were accurately modeled. The visualized flow trajectories, pressure, temperature, and velocity revealed clear patterns. The results were consistent with existing literature and experimental data, validating the method's reliability for design and educational purposes.
- Reverse Flow Detection: The detection of reverse flow at the discharge port confirms operation beyond the designed compression ratio, validating the software's predictive capability.
- Velocity and Leakage Patterns: High-velocity leakage flows (over 200 m/s) were observed at rotor clearances, emphasizing the critical role of geometric precision in minimizing efficiency losses.
- Visualization Tools: Isosurface visualizations provided a detailed 3D understanding of internal flow behavior, supporting engineering insights, while torque and pressure charts provided enhanced interpretation of the internal behavior, pressure distribution, and mechanical load dynamics.
- Tool Versatility: Despite SolidWorks not being a conventional CFD tool for compressor analysis, it proved efficient, accurate, and user-friendly, making it suitable for educational, prototyping, and preliminary design applications.

To conclude, based on the current information, this study is among the first to demonstrate the feasibility of using SolidWorks Flow Simulation for accurate transient CFD modeling of a TSC. The study also introduces reverse flow visualization, torque fluctuation characterization, and isosurface-based 3D interpretation of internal phenomena—offering a practical, accessible CFD alternative for compressor analysis.

Author Contributions: Conceptualization, I.B. and L.C.; methodology, S.M.R.; software, I.B., A.A. and F.D.P.; validation, F.D.P. and A.A.; writing—original draft preparation, A.A., L.C. and I.B.; writing—review and editing, F.D.P., S.M.R. and I.B. All authors have read and agreed to the published version of the manuscript.

Funding: This research received no external funding.

Institutional Review Board Statement: Not applicable.

Informed Consent Statement: Not applicable.

Data Availability Statement: The original contributions presented in this study are included in the article. Further inquiries can be directed to the corresponding author(s).

Conflicts of Interest: The authors declare no conflicts of interest.

References

1. Fleming, J.S.; Tang, Y.; Cook, G. The Twin Helical Screw Compressor Part 1: Development, Applications and Competitive Position. *Proc. Inst. Mech. Eng. Part C J. Mech. Eng. Sci.* **1998**, *212*, 355–367. [CrossRef]
2. Pillis, J.W. Basics of Operation and Application of Oil Flooded Rotary Screw Compressors. In Proceedings of the 28th Turbomachinery Symposium, Houston, TX, USA, 14–16 September 1999; pp. 147–156. [CrossRef]
3. He, Z.; Wang, T.; Wang, X.; Peng, X.; Xing, Z. Experimental Investigation into the Effect of Oil Injection on the Performance of a Variable Speed Twin-Screw Compressor. *Energies* **2018**, *11*, 1342. [CrossRef]
4. Stošić, N. Review Article: Screw Compressors in Refrigeration and Air Conditioning. *HVACR Res.* **2004**, *10*, 233–263. [CrossRef]
5. Wu, W.; Zhang, Z. Development of Single Screw Compressor Technologies and Their Tendency. *Proc. Inst. Mech. Eng. Part E J. Process Mech. Eng.* **2021**, *236*, 738–751. [CrossRef]
6. Ooi, K.T. Twenty Years of Compressor Innovation at NTU, Singapore. In *International Compressor Engineering Conference*; Purdue e-Pubs: West Lafayette, IN, USA, 2014.
7. Stosic, N. On Heat Transfer in Screw Compressors. *Int. J. Heat Fluid Flow* **2015**, *51*, 285–297. [CrossRef]
8. Lysholm, A.J.R. A New Rotary Compressor. *Proc. Inst. Mech. Eng.* **1943**, *150*, 11–16. [CrossRef]
9. Meher-Homji, C.B. The Historical Evolution of Turbomachinery. In Proceedings of the 29th Turbomachinery Symposium, Houston, TX, USA, 18–21 September 2000; American Society of Mechanical Engineers (ASME): New York, NY, USA, 2000; pp. 281–322. [CrossRef]
10. O'Neill, P.A. *Industrial Compressors: Theory and Equipment*; Butterworth-Heinemann: Oxford, UK, 1993.
11. Wang, Y.; Xiong, L.; Feng, D.; Liu, X.; Zhao, S. Research Progress on the Manufacturing of Screw-Shaped Parts in Screw Compressors. *Appl. Sci.* **2024**, *14*, 1945. [CrossRef]
12. Valand, D.; Bhabhor, K.K.; Jani, D.B.; Gandhi, T. Parametric Analysis of a Screw Compressor: A Critical Review. *Int. J. Adv. Res. Sci. Commun. Technol.* **2023**, *3*, 59–71. [CrossRef]
13. Patel, H.H.; Lakhera, V.J. A Critical Review of the Experimental Studies Related to Twin Screw Compressors. *Proc. Inst. Mech. Eng. Part E J. Process. Mech. Eng.* **2020**, *234*, 157–170. [CrossRef]
14. Lu, K.; Sultan, I.A.; Phung, T.H. A Literature Review of the Positive Displacement Compressor: Current Challenges and Future Opportunities. *Energies* **2023**, *16*, 7035. [CrossRef]
15. Cao, F.; Gao, T.; Li, S.; Xing, Z.; Shu, P. Experimental Analysis of Pressure Distribution in a Twin Screw Compressor for Multiphase Duties. *Exp. Therm. Fluid Sci.* **2011**, *35*, 219–225. [CrossRef]
16. Sun, S.; Xing, Z.; Li, Y.; Su, P.C.; Chen, W. Experimental Investigation on Twin Screw Refrigeration Compressor with Different Capacity Control Methods. *Int. J. Refrig.* **2021**, *130*, 370–381. [CrossRef]
17. Liang, X.; Wu, W. Theoretical and Experimental Studies on Oil Injected Twin Screw Air Compressor under Unload Conditions. *IOP Conf. Ser. Earth Environ. Sci.* **2019**, *252*, 032118. [CrossRef]
18. You, C.X. A Theoretical Study of Rotor Forces and Torques in Helical Twin Screw Compressors. Ph.D. Thesis, University of Strathclyde, Glasgow, UK, 1994.

19. Seshaiah, N.; Sahoo, R.K.; Sarangi, S.K. Theoretical and Experimental Studies on Oil Injected Twin-Screw Air Compressor When Compressing Different Light and Heavy Gases. *Appl. Therm. Eng.* **2010**, *30*, 327–339. [CrossRef]
20. Huagen, W.; Ziwen, X.; Pengcheng, S. Theoretical and Experimental Study on Indicator Diagram of Twin Screw Refrigeration Compressor. *Int. J. Refrig.* **2004**, *27*, 331–338. [CrossRef]
21. Giuffrida, A. A Semi-Empirical Method for Assessing the Performance of an Open-Drive Screw Refrigeration Compressor. *Appl. Therm. Eng.* **2016**, *93*, 813–823. [CrossRef]
22. Krichel, S.V.; Sawodny, O. Dynamic Modeling of Compressors Illustrated by an Oil-Flooded Twin Helical Screw Compressor. *Mechatronics* **2011**, *21*, 77–84. [CrossRef]
23. Li, Y.; Liu, Y.; Li, Z.; Wang, C.; Xing, Z.; Ren, D.; Zhu, Y. Semi-Empirical Model of the Twin-Screw Refrigeration Compressor with Capacity Control Devices. *Energy* **2024**, *305*, 132381. [CrossRef]
24. Van Erdeweghe, S.; De Schutter, J.; Van Den Bulck, E. Integral Modeling of a Twin-Screw Compressor. *J. Mech. Des.* **2016**, *138*, 073401. [CrossRef]
25. Lee, W.S.; Ma, R.H.; Chen, S.L.; Wu, W.F.; Hsia, H.W. Numerical Simulation and Performance Analysis of Twin Screw Air Compressors. *Int. J. Rotating Mach.* **2001**, *7*, 65–78. [CrossRef]
26. Wu, Y.-R.; Chi, J.-W. A Numerical Method for the Evaluation of the Meshing Clearance for Twin Screw Rotors with Discrete Tooth Profile Points. *Mech. Mach. Theory* **2013**, *70*, 62–73. [CrossRef]
27. Cavazzini, G.; Giacomel, F.; Benato, A.; Nascimben, F.; Ardizzon, G. Analysis of the Inner Fluid-Dynamics of Scroll Compressors and Comparison between CFD Numerical and Modelling Approaches. *Energies* **2021**, *14*, 1158. [CrossRef]
28. Wang, C.; Wang, B.; Liu, M.; Xing, Z. A Review of Recent Research and Application Progress in Screw Machines. *Machines* **2022**, *10*, 62. [CrossRef]
29. Hammond, J.; Pepper, N.; Montomoli, F.; Michelassi, V. Machine Learning Methods in CFD for Turbomachinery: A Review. *Int. J. Turbomach. Propuls. Power* **2022**, *7*, 16. [CrossRef]
30. Michelassi, V.; Ling, J. Challenges and Opportunities for Artificial Intelligence and High-Fidelity Simulations in Turbomachinery Applications: A Perspective. *J. Glob. Power Propuls. Soc.* **2021**, *2021*, 1–14. [CrossRef]
31. Kovacevic, A. Three-Dimensional Numerical Analysis for Flow Prediction in Positive Displacement Screw Machines. Ph.D. Thesis, City University London, London, UK, 2002.
32. Kovacevic, A. Boundary Adaptation in Grid Generation for CFD Analysis of Screw Compressors. *Int. J. Numer. Meth. Eng.* **2005**, *64*, 401–426. [CrossRef]
33. Basha, N.; Kovacevic, A.; Rane, S. Analysis of Oil-Injected Twin-Screw Compressor with Multiphase Flow Models. *Designs* **2019**, *3*, 54. [CrossRef]
34. Rane, S.; Kovačević, A.; Stošić, N. Grid Generation for CFD Analysis and Design of a Variety of Twin Screw Machines. *Designs* **2019**, *3*, 30. [CrossRef]
35. Yeoh, G.H.; Barber, T. Assessment of Interface Capturing Methods in Computational Fluid Dynamics (CFD) Codes—A Case Study. *J. Comput. Multiph. Flows* **2009**, *1*, 201–215. [CrossRef]
36. Andres, R.; Hesse, J.; Hetze, F.; Low, D. Cfd Simulation of a Two Stage Twin Screw Compressor Including Leakage Flows and Comparison with Experimental Data. *IOP Conf. Ser. Mater. Sci. Eng.* **2018**, *425*, 012018. [CrossRef]
37. Malael, I.; Petrescu, V. Computational Fluid Dynamics Evaluation of an Oil-Flooded Screw Compressor. *Eng. Technol. Appl. Sci. Res.* **2023**, *13*, 11533–11539. [CrossRef]
38. Chamoun, M.; Rulliere, R.; Haberschill, P.; Peureux, J.-L. Modelica-Based Modeling and Simulation of a Twin Screw Compressor for Heat Pump Applications. *Appl. Therm. Eng.* **2013**, *58*, 479–489. [CrossRef]
39. Papes, I.; Degroote, J.; Vierendeels, J. 3D CFD Analysis of an Oil Injected Twin Screw Expander. In Proceedings of the Volume 6A: Energy, San Diego, CA, USA, 15 November 2013; American Society of Mechanical Engineers: New York, NY, USA, 2014; p. V06AT07A040. [CrossRef]
40. Di Mattia, E.; Gambarotta, A.; Morini, M.; Saletti, C. Application of Modelling Approaches of Twin-Screw Compressors: Thermodynamic Investigation and Reduced-Order Model Identification. *E3S Web Conf.* **2021**, *312*, 05001. [CrossRef]
41. Xueming, H.; Jin, D.; Meiping, W.; Hongyuan, L.; Chenggang, L. The Three-Dimensional Numerical Simulation and Experimental Research on Screw Compressor. *Adv. Mech. Eng.* **2015**, *7*, 189579. [CrossRef]
42. Byeon, S.-S.; Lee, J.-Y.; Kim, Y.-J. Performance Characteristics of a 4 × 6 Oil-Free Twin-Screw Compressor. *Energies* **2017**, *10*, 945. [CrossRef]
43. Casari, N.; Fadiga, E.; Pinelli, M.; Suman, A.; Ziviani, D. CFD Simulations of Single- and Twin-Screw Machines with OpenFOAM. *Designs* **2020**, *4*, 2. [CrossRef]
44. Bojko, M.; Hertl, L.; Drabkova, S. Methods of CFD Modelling of Twin-Screw Pumps for Non-Newtonian Materials. *MM Sci. J.* **2021**, *2021*, 5366–5372. [CrossRef]
45. Dragan, V.; Malael, I.; Gherman, B. A Comparative Analysis Between Optimized and Baseline High Pressure Compressor Stages Using Tridimensional Computational Fluid Dynamics. *Eng. Technol. Appl. Sci. Res.* **2016**, *6*, 1103–1108. [CrossRef]

46. Aydın, A.; Engin, T.; Kovacevic, A. Design Optimisation of a Screw Compressor with a Focus on Rotor Depth: A Computational Fluid Dynamics Approach. *Int. J. Refrig.* **2025**, *170*, 385–397. [CrossRef]
47. Lyu, W.; Luzi, G.; Delgado, A.; Schellin, T.E. CFD Analysis of Lab-Scale Prototypes Two-Phase Fluid Flow Twin-Scroll Compressor and Expander. *Energy* **2025**, *314*, 134192. [CrossRef]
48. Khaleel, H.H. Structural Analysis of Compressor Blades Using Finite Elements Method. *Math. Model. Eng. Probl.* **2023**, *10*, 695–700. [CrossRef]
49. Khalid, A.; Mandzyuk, V. Optimization of High-Bypass Turbofan High-Pressure Compressor Blade—A Case Study. *Kennesaw J. Undergrad. Res.* **2024**, *11*, 4. [CrossRef]
50. Mykhailiuk, V.; Zasadzień, M.; Liakh, M.; Deineha, R.; Mosora, Y.; Faflei, O. Analysis of the Possibility of Modeling Gas Separators Using Computational Fluid Dynamics. *Manag. Syst. Prod. Eng.* **2024**, *32*, 80–86. [CrossRef]
51. Popescu, F.D.; Radu, S.M.; Andraş, A.; Kertész Brînaş, I. A Grafo-Numeric Method of Determination of the Operation Power of the Rotor of EsRc-1400 Bucket Wheel Excavator Using Computer Simulation in SolidWorks. *MATEC Web Conf.* **2019**, *290*, 04007. [CrossRef]
52. Popescu, F.D.; Radu, S.M.; Andras, A.; Brinas, I.; Marita, M.-O.; Radu, M.A.; Brinas, C.L. Stability Assessment of the Dam of a Tailings Pond Using Computer Modeling—Case Study: Coroieşti, Romania. *Appl. Sci.* **2023**, *14*, 268. [CrossRef]
53. Radu, S.M.; Popescu, F.D.; Andraş, A.; Andraş, I.; Brînaş, I.; Vâlceanu, F. Numerical analysis of fatigue for the assessment of remaining service life of the ERc 1400-30/7 bucket wheel excavator. *Proc. Rom. Acad. Ser. A* **2021**, *22*, 143–152.
54. Wu, H.; Huang, H.; Zhang, B.; Xiong, B.; Lin, K. CFD Simulation and Experimental Study of Working Process of Screw Refrigeration Compressor with R134a. *Energies* **2019**, *12*, 2054. [CrossRef]
55. Singh, G.; Sun, S.; Kovacevic, A.; Li, Q.; Bruecker, C. Transient flow analysis in a Roots blower: Experimental and numerical investigations. *Mech. Syst. Signal Process.* **2019**, *134*, 106305. [CrossRef]
56. Ding, H.; Jiang, Y. CFD simulation of a screw compressor with oil injection. *IOP Conf. Ser. Mater. Sci. Eng.* **2017**, *232*, 012020. [CrossRef]
57. Stosic, N.; Smith, I.K.; Kovacevic, A. *Screw Compressors: Mathematical Modelling and Performance Calculation*; Springer: Berlin/Heidelberg, Germany, 2005. [CrossRef]
58. Kovacevic, A.; Stosic, N.; Smith, I. *Screw Compressors: Three Dimensional Computational Fluid Dynamics and Solid Fluid Interaction*; Springer: Berlin/Heidelberg, Germany, 2007. [CrossRef]

Disclaimer/Publisher's Note: The statements, opinions and data contained in all publications are solely those of the individual author(s) and contributor(s) and not of MDPI and/or the editor(s). MDPI and/or the editor(s) disclaim responsibility for any injury to people or property resulting from any ideas, methods, instructions or products referred to in the content.